

Longitudinal fields in electromagnetic waves

V.G. Niziev, A.V. Nesterov

Institute on Laser and Information Technologies of Russian Academy of Sciences
Shatura, Moscow Region, 140700, RUSSIA, e-mail: niziev@laser.ru

Abstract

The structure and properties of the longitudinal field in electromagnetic waves have been studied in the case of the superposition of plane waves, in cylindrical and spherical modes. It has been ascertained that the phase velocity of the longitudinal field is directed along the field vector. Another feature is the $\pi/2$ phase shift of the longitudinal electrical field relative to the magnetic field preventing the energy transport by this field. The analytical method for the theoretical description of the radially and azimuthally polarized beams is presented. It does not have any inherent contradictions. The longitudinal field is formed with the radial component of the wave vectors directed to the axis of the beam. Coherent superposition of two equal contradirectional radially or azimuthally polarized beams gives a special point in the waist. All three field components including the longitudinal field equal zero at this point. It was shown that in the spherical high order modes, the radius of zero-field area in the sphere center increases proportional to the mode order.

1. Introduction

The classical papers describing the transversal laser beam structure of the open resonators have been well known [1]. Laguerre-Gaussian modes TEM_{pq} (the indexes indicate the number of nodes in the radial and azimuthal directions) belong to the self-reproducing solutions of the wave equation in the cylindrical coordinates. The obtained field distributions are in good agreement with the experimentally observed mode structure of laser beams. The theoretical field distributions were calculated on the basis of the scalar wave equation and correspond to the homogeneously polarized beams: the direction of the electric field in every point of the beam cross section remains the same.

In early works on laser resonators, the authors already pointed out that the coherent superposition of two modes TEM_{01} can lead to the generation of modes with inhomogeneous polarization, such as radially, azimuthally or some others. The method of the outside cavity superposition of linearly polarized modes for obtaining inhomogeneously polarized modes (IPM) with the use of the interferometer is widespread today.

There has been considerable interest recently in IPM, based on the perspectives of the application of such modes and on the appearance of new methods of their generation. Radially and azimuthally polarized modes, possessing axially symmetry of all parameters including polarization are the most promising. There are many articles discussing the practical applications of inhomogeneously polarized modes. Radially polarized beams have been proposed for the laser cutting of metals [2] and azimuthal polarization for hole punching [3]. The radially polarized beam appears more efficient than a linearly polarized beam in experiments on laser heating plasma, due to its higher resonance absorption [4]. The authors of [5, 6] proved that a radially polarized beam can be focused more sharply than a linearly polarized beam. These modes can be applied for trapping cold atoms [7], and the helical modes are proposed in diagnostic and metrological systems [8].

While studying IPM, special attention has been paid to the longitudinal field component, directed parallel to the electromagnetic wave propagation direction. In spite of the insufficient understanding of the physical nature of the longitudinal field, the first experiments to detect it have been already conducted [9, 10, 11]. There are also some suggestions about the practical use of this field component. The longitudinal component of an electric field for a sharply focused radially polarized beam can be used for the acceleration of relativistic electrons [12, 13].

Some problems, however, have arisen with the theoretical description of the IPM [14]. The reason is that the classical solutions for homogeneously polarized Laguerre-Gaussian modes [1]

contradict the Maxwell's equation $\nabla \cdot \mathbf{E} = 0$, which makes impossible the exact definition of application limits of such approach. The classical solutions contain also other limits, which reduce their relevance to describing inhomogeneously polarized modes. The longitudinal field is neglected by describing the paraxial beams. By the sharp focusing of IPM, the longitudinal field should be taken into account, because the longitudinal field possesses a maximum amplitude in the region, where the propagated field component equals to zero.

Debye approximation is used for describing the longitudinal field at the sharp focusing [10,15,16,17], which allows for calculating field components at the focal plane. The numeric solution of Maxwell's equations is an exact description method for electromagnetic fields [18]. In spite of the detail and certain advantages of such solutions, especially in complicated geometries, they are not quite convenient for revealing characteristic physical features of the phenomena like the longitudinal field in our case.

The purpose of the present work is the study of the structure and properties of the longitudinal fields in the case of the superposition of plane waves, in cylindrical and spherical modes. Considering the electromagnetic waves in these different geometries by the use of analytical formulae, the general significant features of the longitudinal field are studied as an important element of the wave process.

2. Superposition of the plane waves

Some physical features, which are important for studying the cylindrical and spherical modes, can be considered by the vector superposition of the plane waves crossing each other at non-zero angle (Fig. 1). The wave vectors of the interfering waves and their electric field vectors are assumed to lie in the x-z plane and the angle between axis z and the wave vectors equals $\pm\theta$. These waves are described by following expression:

$$\mathbf{E}_{1,2} = (\mathbf{e}_x E_0 \cos \theta \mp \mathbf{e}_z E_0 \sin \theta) \exp[i(\pm kx \sin \theta + kz \cos \theta) - i\omega t]$$

where E_0 is the field amplitude that is the same for both waves. The upper signs correspond to the wave with the index 1, the lower signs to the wave with index 2. The addition of the corresponding field components gives the formula for the resulting wave:

$$\begin{aligned} E_x &= 2E_0 \cos \theta \cos(kx \sin \theta) \exp(ikz \cos \theta - i\omega t) \\ E_z &= 2iE_0 \sin \theta \sin(kx \sin \theta) \exp(ikz \cos \theta - i\omega t) \end{aligned} \quad (1)$$

The magnetic field of the waves is directed parallel to the axis y and perpendicular to the plane of the drawing. The resulting magnetic field has only one component:

$$H_y = 2H_0 \cos(kx \sin \theta) \exp(ikz \cos \theta - i\omega t) \quad (2)$$

The field components E_x and H_y build a running wave with the wave vector parallel to the z-axis. Since the averaged Poynting vector, calculated for these components, does not equal zero, the energy is transported along the wave vector. A characteristic interferometric dependence $\cos(kx \sin \theta)$ is considered along the axis x, obtained through the addition of the equally directed components E_x .

In spite of the same structure of the formulae for E_x and E_z , the field has some differences. The direction of E_z is parallel to the phase velocity of this field. Another feature is the imaginary unit in the expression for E_z . It means the $\pi/2$ phase shift of the field E_z is relative to H_y . The average Poynting vector equals zero for the components E_z and H_y . No energy is transported in this case. This effect is attributed to the fact that the wave vector components of the interfering waves associated with the E_z are directed along axis x in the opposite direction.

In the particular case $\theta=0$, the traveling wave is obtained from formulae (1) and (2): $E_x = H_y = 2E_0 \exp(ikz - i\omega t)$; $E_z=0$. For $\theta=90^\circ$, the formula for the standing wave is valid: $E_x = 0$; $E_z = 2iE_0 \sin(kx) \exp(-i\omega t)$; $H_y = 2H_0 \cos(kx) \exp(-i\omega t)$.

The taking into account of the arbitrary phase shift between the interfering wave does not change the above described qualitative features. If the electric field of the interfering waves is

directed parallel to the axis y , the solutions will be obtained with the mutual substitution between E and H in formulae (1) and (2). In this case, the magnetic field has a component directed along axis z , which does not contribute to the energy transport. In common cases, the distribution of such fields can be rather complicated. Nevertheless, they appear as an important element in the wave processes.

The common traveling and standing electromagnetic waves are transversal. The wave vector and the electric and magnetic vectors are mutually perpendicular, and the phase velocity direction coincides with the wave vector. But in the considered case, E_z does not participate in the energy transfer. The time averaged wave vector equals zero. The formula (1) for E_z includes the exponential term, determining the direction of the phase velocity along the components E_z . This field component is called the longitudinal field.

The longitudinal field is an indispensable part practically of all wave processes, excepting most idealized cases like traveling or standing plane waves. According to formula (1), the field ratio E_x/E_z can vary from zero to infinite depending on the mutual angle of the interfering waves.

If wave (1) composing of waves 1 and 2 (Fig.1) is directed opposite to the same wave with the equal amplitude, a standing wave will be obtained with a two-dimensional interfering pattern in the x - z plane. The corresponding expressions for E_x , E_z , H_y components can be obtained as a superposition of the solutions (1) and (2) written for z and $-z$:

$$\begin{aligned} E_x &= 4i E_0 \cos \theta \cos(kx \sin \theta) \sin(kz \cos \theta) \exp(-i\omega t) \\ E_z &= 4i E_0 \sin \theta \sin(kx \sin \theta) \cos(kz \cos \theta) \exp(-i\omega t) \\ H_y &= 4 H_0 \cos(kx \sin \theta) \cos(kz \cos \theta) \exp(-i\omega t) \end{aligned} \quad (3)$$

The distributions for the fields E_x and E_z are shifted in the plane x - z . The lobes of one field overlap the knots of the other one. An analogical situation will be observed for the spherical modes in paragraph 4. Other properties of the fields E_x and E_z in standing wave (3) are equal. Both components possess a $\pi/2$ phase shift relative to the magnetic field and thus do not transport the energy. Actually, the energy currents of the traveling waves, forming the interference pattern, are compensated.

The physical nature of the longitudinal field has been considered in the present paragraph by the use of the simple example of interfering ideal plane waves. The spatially confined longitudinal fields will be studied in the laser beams and spherical modes in the next paragraphs.

3. The longitudinal field in cylindrical modes

The radially and azimuthally polarized beams are considered as the most interesting examples of the inhomogeneously polarized modes by use of the analytical method without contradictions to Maxwell's equations.

It is known that the introduction of the wave equation leads to the exact formal reduction of the initial Maxwell's equations. Instead of the four vector equations for the electric and magnetic fields, two equations are solved for the example of the magnetic field:

$$\Delta \mathbf{H} + k^2 \mathbf{H} = 0, \quad \nabla \cdot \mathbf{H} = 0, \quad (4)$$

The components of the electric field are calculated from the solution for the magnetic field according to Maxwell's equation:

$$\nabla \times \mathbf{H} - \frac{1}{c} \dot{\mathbf{E}} = 0 \quad (5)$$

As previously mentioned, the solution of the scalar wave equation under assumption of linear polarization leads to contradiction with the equation $\nabla \cdot \mathbf{E} = 0$ [14].

To consider the general properties of the equation system (4) concerning the longitudinal field, the modes with axially symmetric polarization are chosen as its solution:

$\mathbf{H}=\mathbf{H}(\rho,z)=H_\rho(\rho,z)\mathbf{e}_\rho+H_\phi(\rho,z)\mathbf{e}_\phi+H_z(\rho,z)\mathbf{e}_z$. The equation system decays into one scalar equation for the azimuthal component and three other scalar equations for the radial and longitudinal fields. The following equation is valid for the azimuthally polarized component:

$$\frac{1}{\rho} \frac{\partial}{\partial \rho} \left(\rho \frac{\partial H_\phi}{\partial \rho} \right) + \frac{\partial^2 H_\phi}{\partial z^2} + \left(k^2 - \frac{1}{\rho^2} \right) H_\phi = 0 \quad (6)$$

The direct substitution of $\mathbf{H}=\mathbf{H}_\phi(\rho,\phi,z)\cdot\mathbf{e}_\phi$ in the equation system (4) leads to the conclusion about axially symmetry of the azimuthally polarized mode. Thus, the solution of the equation (6) has the form $\mathbf{H}=\mathbf{H}_\phi(\rho,z)\cdot\mathbf{e}_\phi$ which satisfies Maxwell's equation $\nabla\cdot\mathbf{H}=0$.

In the paraxial approximation assuming

$$H_\phi(\rho, z) \rightarrow H_\phi(\rho, z) \exp(ikz),$$

the expression for the ρ - z part of the Laguerre-Gaussian modes TEM_{pq} by $q = 1$:

$$H_\phi = \sqrt{\frac{2}{\pi}} \frac{1}{\sqrt{p+1}} \cdot \frac{1}{w} \cdot (\sqrt{2} \cdot R) \cdot L_p^1(2 \cdot R^2) \cdot \exp(-R^2) \cdot \exp(i\theta) \quad (7a)$$

$$\theta = 2\arctg Z - 2Z \frac{z_0^2}{w_0^2} - ZR^2; \quad R = \rho/w; \quad R_0 = \rho/w_0; \quad Z = z/z_0; \quad z_0 = \frac{\pi w_0^2}{\lambda}; \quad w^2 = w_0^2 \cdot (1 + Z^2)$$

$$L_p^1(x) = \sum_{m=0}^p (-1)^m \frac{(p+1)!}{(p-m)!(m+1)! m!} x^m$$

The components of the electric field are calculated according to (5) by $z = 0$ and have the form:

$$E_\rho \approx H_\phi = \frac{2}{\sqrt{\pi}} \frac{1}{\sqrt{p+1}} \frac{1}{w_0} R_0 L_p^1(2 \cdot R_0^2) \exp(-R_0^2) \quad (7b)$$

$$E_z = i \frac{1}{\pi \sqrt{\pi}} \frac{\lambda}{w_0} \frac{1}{w_0} \sqrt{(p+1)} \exp(-R_0^2) \left[L_p(2R_0^2) + L_{p+1}(2R_0^2) \right] \quad (7c)$$

The distribution of the field components E_r and H_ϕ are approximately equal under the condition: $\frac{\lambda^2}{\pi^2 w_0^2} \ll 1$.

The longitudinal field component E_z has some characteristic features.

- ✚ The maximum of the longitudinal field locates at the beam axis, where the radial component equals zero.
- ✚ The longitudinal field has the additional factor λ/w_0 which determines its value relative to H_ϕ and E_ρ .
- ✚ The imaginary unit in the expression for E_z implies the $\pi/2$ phase shift relative to the magnetic field. Thus, by analogy to the case with the interfering plane waves, the longitudinals do not participate in the energy transfer.

The field distribution for H_ϕ and E_z are shown in Fig. 1 for radially polarized modes R-TEM_{p1^*} ($p=0, 1, 2$).

The calculation method conducted for the azimuthal field is not applicable for the radial polarization. Actually, the form $\mathbf{H}=\mathbf{H}_\rho(\rho,z)\cdot\mathbf{e}_r$ contradicts the equation $\nabla\cdot\mathbf{H}=0$. So there is only one case of the "single component" solution for magnetic field not contradicting Maxwell's equations, which corresponds to the axially symmetric field with azimuthal direction $H_\phi(r,z)$. The complete solution has three components $H_\phi(r,z)$, $E_r(r,z)$, $E_z(r,z)$. Thanks to the symmetry of Maxwell's equations the same statement can be made for the electric field. In this case, the solution has the components $E_\phi(r, z)$, $H_r(r,z)$, $H_z(r,z)$.

The presented method can be extended to the Debye approximation used for the calculation of the field at the focal plane of a lens [10,11,15,16]:

$$H_{\varphi}(\rho, z \approx 0) = k \int_0^{\theta_1} H_{\varphi 0}(f \sin \alpha) \sqrt{\cos \alpha} J_1(k \rho \sin \alpha) \exp(i k z \cos \alpha) \sin \alpha d\alpha \quad (8a)$$

$$E_r(\rho, z \approx 0) = -k \int_0^{\theta_1} H_{\varphi 0}(f \sin \alpha) \sqrt{\cos \alpha} J_1(k \rho \sin \alpha) \exp(i k z \cos \alpha) \sin \alpha \cos \alpha d\alpha \quad (8b)$$

$$E_z(\rho, z \approx 0) = -i \cdot k \int_0^{\theta_1} H_{\varphi 0}(f \sin \alpha) \sqrt{\cos \alpha} J_0(k \rho \sin \alpha) \exp(i k z \cos \alpha) \sin^2 \alpha d\alpha \quad (8c)$$

Here θ_1 is the angle of aperture of the optical system and f the focal length. The Debye approximation describes the field only in the narrow region along the axis z at the focus. Analogue formulae can be obtained if azimuthal polarization is assumed for the electrical field, leading to the field components $E_{\varphi}(\rho, z \approx 0)$, $H_{\rho}(\rho, z \approx 0)$, $H_z(\rho, z \approx 0)$. The azimuthally polarized electrical field $E_{\varphi 0}(\rho)$ is taken in this case as the initial field.

The following qualitative description of formatting the longitudinal field can be conducted on the base of the formulae (8). Like the case of the interfering plane waves, the wave vectors of the beam directed from the collecting lens to the focus can be decomposed into two components: the parallel and the perpendicular to the lens axis. The parallel components of the wave vectors form the running wave. This wave has a ring amplitude distribution and radial field component.

The radial wave vector components, directed to the beam axis, form the longitudinal field with a maximum at the beam axis. The radial size of the longitudinal field is determined by diffraction. After the focus, the longitudinal field transforms into the diverging wave.

The characteristic feature of the considered beams is that the running wave and the longitudinal field have quite different, only partly overlapping field distributions. The longitudinal field E_z has a maximum at the beam axis, where E_r equals zero and, vice versa, E_z is relatively small in the maximum of the field E_r . This fact reveals the possibility of independent influence on one of the field components. Such influence could be realised through the absorption or reflection of the chosen field component.

Let us consider the case of the coherent superposition of the two directed-in-opposite directions equal beams using two lenses with the shared focus. Assuming a zero phase shift, the resulting fields components will be determined by the sum for E_r component: $E_r(\rho, z \approx 0) + E_r(\rho, -z \approx 0)$ and the subtraction for H_{φ} and E_z components: $H_{\varphi}(\rho, z \approx 0) - H_{\varphi}(\rho, -z \approx 0)$ and $E_z(\rho, z \approx 0) - E_z(\rho, -z \approx 0)$ respectively.

The obtained standing wave has the form:

$$H_{\varphi}(\rho, z \approx 0) = 2ik \int_0^{\theta_1} H_{\varphi 0}(f \sin \alpha) \sqrt{\cos \alpha} J_1(k \rho \sin \alpha) \sin(kz \cos \alpha) \sin \alpha d\alpha \quad (9a)$$

$$E_r(\rho, z \approx 0) = -2k \int_0^{\theta_1} H_{\varphi 0}(f \sin \alpha) \sqrt{\cos \alpha} J_1(k \rho \sin \alpha) \cos(kz \cos \alpha) \sin \alpha \cos \alpha d\alpha \quad (9b)$$

$$E_z(\rho, z \approx 0) = 2k \int_0^{\theta_1} H_{\varphi 0}(f \sin \alpha) \sqrt{\cos \alpha} J_0(k \rho \sin \alpha) \sin(kz \cos \alpha) \sin^2 \alpha d\alpha \quad (9c)$$

It is apparent from (9) that the field components H_{φ} and E_z possess knots, and E_r has a lobe in the focal plane. At the same time, E_r is always equal to zero on the beam axis. A unique situation appears in the point on the beam axis in the focal plane: all the free field components equal zero. This peculiarity will be considered in detail in the next paragraph.

4. Longitudinal fields in spherical mode

In spherical coordinates, the physical situation is like that in cylinder coordinates. For the description of a physical object, we can use a mathematical solution of the scalar wave equation in spherical coordinates [19-20] (for example for magnetic field) only if this solution satisfies the equation $\nabla \cdot \mathbf{H} = 0$. By analogy with the tasks of Part 3, the solution is chosen in the form of the axially symmetric azimuthally polarized mode $\mathbf{H} = H_\varphi(r, \theta) \cdot \mathbf{e}_\varphi$. The equation $\nabla \cdot \mathbf{H} = 0$ is satisfied and the vector wave equation is reduced to the scalar:

$$\frac{1}{r^2} \frac{\partial}{\partial r} \left(r^2 \frac{\partial H_\varphi}{\partial r} \right) + \frac{1}{r^2 \sin \theta} \frac{\partial}{\partial \theta} \left(\sin \theta \frac{\partial H_\varphi}{\partial \theta} \right) - \frac{H_\varphi}{r^2 \sin \theta} + k^2 H_\varphi = 0$$

The general solution of this equation has the form:

$$H_\varphi(r, \theta) = \text{Const} \cdot P_n^1(\cos \theta) \cdot j_n(kr) \quad (10a)$$

Here P_n^1 is an associated Legendre polynomial of the second kind, and j_n the spherical Bessel function of the first kind. The choice of the Bessel function determines a standing wave as a superposition of the spherical convergent and divergent waves.

The component of the electrical field are found according to (5):

$$E_r(r, \theta) = -C i n(n+1) j_n(kr) \frac{1}{kr} P_n(\cos \theta) \quad (10b)$$

$$E_\theta(r, \theta) = -C i P_n^1(\cos \theta) \left[\frac{n+1}{2n+1} j_{n-1}(kr) - \frac{n}{2n+1} j_{n+1}(kr) \right] \quad (10c)$$

Here $P_n = P_n^0$, C is a constant. Since the solutions represent a standing wave, both components possess a $\pi/2$ phase shift relative to the magnetic field. It is obvious that the radial component of the electrical field E_r would be a longitudinal field in the case of the spherical traveling wave.

The constant C can be expressed through the constant energy current P_{rad} of the convergent or divergent wave at the large r :

$$P_{\text{rad}} = c_0 \int_0^\pi 2\pi(r \sin \theta) \cdot (E_\theta^2(r, \theta) + H_\varphi^2(r, \theta)) \cdot (r d\theta), \quad (11)$$

where c_0 is the light speed.

Using the asymptotic formula for spherical Bessel functions:

$$j_n(kr) \rightarrow \frac{1}{kr} \sin\left(kr - n \frac{\pi}{2}\right),$$

$r \rightarrow \infty$

the fields H_φ and E_θ can be expressed as:

$$H_\varphi(r, \theta) = C P_n^1(\cos \theta) \cdot \frac{1}{kr} \sin\left(kr - n \frac{\pi}{2}\right) \quad r \rightarrow \infty$$

$$E_\theta(r, \theta) = C i P_n^1(\cos \theta) \frac{1}{kr} \cos\left(kr - n \frac{\pi}{2}\right) \quad r \rightarrow \infty.$$

Applying the formula

$$\int_{-1}^1 [P_n^1(x)]^2 dx = \frac{n(n+1)}{2n+1},$$

for the calculation of the integral in (11), the following expression for the constant C is obtained:

$$P_{\text{rad}} = 2\pi \frac{C^2}{k^2} c_{\text{light}} \frac{n(n+1)}{2n+1}. \quad (12)$$

It is clear from the physical point of view that all three field components H_ϕ , E_r , E_θ should be equal to zero in the center of the sphere. This fact determines the choice of the mode index $n = 2, 3, 4, \dots$. The field distribution over the polar angle is described by Legendre polynomials and shown in Fig. 3. It should be noted that the number of petals increases with the increasing mode number, but the spatial localization of field components differs. The maximum of the E_r is located at the poles, while the maximum of H_ϕ and E_θ equals zero at the polar axis.

The radial dependence of the field components H_ϕ , E_r , E_θ is presented in Fig. 4. The modes for $n=2$ and $n=16$ are so scaled to underline a quantitative feature of the shown distributions. The radius of the zero-field area in the centre of the sphere grows with the mode number. This behaviour of the field means that the mode of higher orders does not penetrate into the sphere of radius $r_0 \sim nk$.

Another feature of the presented distribution is that the field E_r decreases along the radius stronger than the components H_ϕ and E_θ as determined by the multiplier $1/kr$ in the expression for E_r . The integrals of the energy density over the space for the field components H_ϕ and E_θ do not converge. On the contrary, the energy density of the radial component E_r can be integrated:

$$W_{\text{non}} = \int_0^\pi \int_0^\infty 2\pi r^2 \sin \theta [E_r(r, \theta)]^2 d\theta dr.$$

The field E_r is practically localized in a spherical envelope, whose radius and thickness increase with the mode number. Fig. 5 depicts this fact for the modes of different orders. The phase distribution of the fields E_θ and E_r in the cross section of the sphere parallel to the polar axis is shown in Fig. 6. The spherical modes retain the phase properties of the TEM modes in the cylindrical coordinates, namely the relative π phase shift between the neighbour mode fragments separated by the zero knot.

Fig. 7 shows the dependence of the maximum field value in a mode on the mode number for all three field components. The expression (12) is used for the constant C . The equal energy current is assumed in the calculation. Fig. 5 demonstrates well the location of the field maximum. This maximum for the longitudinal field is always located on the polar axis. The maximum field value for the longitudinal field is larger than the corresponding values for H_ϕ and E_θ independent of the mode number. The radial coordinate r_{max} relating to the maximum field value in a mode can be determined from the simple relation $kr_{\text{max}} \approx n$.

The solution of the wave equation in spherical coordinates be modelled experimentally by the use of the laser radiation. Powerful lasers are usually systems with large apertures, and their beams possess many mode transversal strictures. Modern diffraction mirrors with high polarization selectivity can force the laser to generate radially polarized high order single transverse mode [21]. The focusing counter propagating waves of such modes can approach the spherical mode with strong longitudinal fields. The exposition of spherical targets to such a longitudinal field would be interesting from the point of view of the radiation absorption or acceleration of the relativistic electrons.

5. Conclusion

The structure and properties of the longitudinal field in electromagnetic waves has been studied in the case of the superposition of plane waves, in cylindrical and spherical modes. The longitudinal field is an indispensable part practically of all wave processes, excepting most idealized cases like traveling or standing plane waves.

The analytical formulae give the general significant features of the longitudinal field. The ratio between the longitudinal and transversal fields can vary from zero to infinite depending on the mutual angle of the interfering waves. The phase velocity of the longitudinal field is directed along

the field vector. Another feature is the $\pi/2$ phase shift of the longitudinal electrical field relative to the magnetic field, preventing the energy transport by this field.

It has been shown there is a single one-component solution of the scalar wave equation in the cylinder and spherical coordinates satisfying Maxwell's equations. It is the azimuthally polarized modes with axially symmetric field distribution. The analytical method for the theoretical description of the radially and azimuthally polarized beams has been presented. It does not have any inherent contradictions. The longitudinal field is formed with the radial component of the wave vectors directed to the axis of the beam. The radial size of longitudinal field is determined by diffraction. The longitudinal field transforms into the diverging wave after focus.

Coherent superposition of two contradirectional beams gives a special point at the waist. All three field components, including the longitudinal field, equal zero at this point. It was shown that in the spherical high order modes, the radius of zero-field area r_0 at the sphere center increases proportional to the mode order $r_0 \sim n/k$.

References

1. S. Solimeno, B. Crosignani, P. DiPorto, "Guiding, Diffraction and Confinement of Optical Radiation" (Academic Press, New York, 1986).
2. V. G. Niziev, A. V. Nesterov, "Influence of Beam Polarization on Laser Cutting Efficiency," *J. of Phys. D: Appl. Phys.* 32, 1455-1461 (1999).
3. M. Meier, H. Glur, E. Wyss, Th. Feurer, V. Romano, "Laser Microhole Drilling Using Q-Switched Radially and Tangentially Polarized Beams," *Proc. of SPIE* 6053, 313-318 (2005).
4. A. V. Nesterov, V. G. Niziev, "Laser Beams with Axially Symmetric Polarization," *J. of Phys. D: Appl. Phys.* 33, 1817-1822 (2000).
5. R. Dorn, S. Quabis, And G. Leuchs, "Sharper Focus for a Radially Polarized Light Beam," *Phys. Rev. Lett.* 91, 233901 (2003).
6. C. J. R. Sheppard, A. Choudhury, "Annular Pupils, Radial Polarization, and Superresolution," *Appl. Opt.* 43, 4322-4327 (2004).
7. A. V. Bezverbnny, V. G. Niziev, A. M. Tumaikin, "Dipole Traps for Neutral Atoms Formed by Nonuniformly Polarised Laguerre Modes," *Quantum Electronics* 34, 685-689 (2004).
8. T. I. Arsenyan, N. N. Fedotov, L. S. Kornienko, P. V. Korolenko, E. A. Kulyagina, G. V. Petrova, "Laser Beam with Helical Wavefront Dislocations and their Applications in the Diagnostical and Metrological Systems," *SPIE* 2713, 453 (1995).
9. Godai Miyaji, Noriaki Miyanaga, Koji Tsubakimoto, Keiichi Sueda, and Ken Ohbayashi "Intense longitudinal electric fields generated from transverse electromagnetic waves," *Applied Physics Letters* 84, 19 (2004) p.3855-3857
10. S. Quabis, R. Dorn, M. Eberler, O. Glöckl, G. Leuchs, "The focus of light – theoretical calculations and experimental tomographic reconstruction," *Appl. Phys. B* 72, 109-113 (2001)
11. G. K. Rurimo, M. Schardt, S. Quabis, S. Malzer, Ch. Dotzler, A. Winkler, G. Leuchs, G. H. Döhler, D. Driscoll, M. Hanson, A. C. Gossard, S. F. Pereira. "Using a quantum well heterostructure to study the longitudinal and transverse electric field components of a strongly focused laser beam," *Journal of Applied Physics* **100**, 023112, 2006.

12. S. C. Tidwell, D. H. Ford, W. D. Kimura, "Generating Radially Polarized Beams Interferometrically," *Appl. Opt.* 29, 2234-2239 (1990).
13. S. C. Tidwell, G. H. Kim, W. D. Kimura, "Efficient Radially Polarized Laser Beam Generation with a Double Interferometer," *Appl. Opt.* 32, 5222-5229 (1993).
14. Lax M, Louisell W H and Mc Knight W B 1975. "From Maxwell to paraxial wave optics," *Phys. Rev. A* 11 1365–70
15. A.V. Nesterov, V. G. Niziev, "Propagation Features of Beams with Axially Symmetric Polarization," *J. Opt. B: Quantum and Semiclassical Opt.* 3, 215-219 (2001).
16. Stamnes J J 1986. "Waves in Focal Regions The Adam Hilger Series on Optics and Optoelectronics" (Bristol: Institute of Physics Publishing)
17. Yuichi Kozawa and Shunichi Sato. "Focusing Properties of a double-ring-shaped radially polarized beam," *Optics Letters* 31, 6, p. 820-822, 2006.
18. A. Taflove and S.C. Hagness. "The Finite-Difference Time-Domain Method". *Computational Electrodynamics* (Artech House, Boston, 2000).
19. M. Abramowitz and I. Stegun eds., *Handbook of Mathematical functions with Formulas, Graphs and Mathematical Tables*, National Bureau of Standards. Washington, D. C., 1964.
20. Riley, K.F., Hobson, M.P., and Bence, S.J. (2002). *Mathematical methods for physics and engineering*, Cambridge University Press.
21. A. V. Nesterov, V.G. Niziev, and V.P. Yakunin, "Generation of high-power radially polarized beam," *J. Phys. D: Appl. Phys.* **32**, 2871-2875 (1999).

Captions

1. The interference of the two plane waves. Arrows show directions of the wave vectors and electric and magnetic fields.
2. The calculated distributions of longitudinal components of electric field E_z and azimuthally directed magnetic field H_ϕ in the waist for the radially polarized modes of different orders.
3. The distribution of field components H_ϕ , E_r , E_θ in coordinates: azimuthal-polar angles. The three pictures correspond to different mode orders n .
4. The radial part of the distribution of field components H_ϕ , E_r , E_θ for different mode orders n . The scale for two curves is not correlated.
5. Contour type pictures of the distribution of amplitude of field components H_ϕ , E_r , E_θ in the coordinates: polar angle – radius for the modes of different orders.
6. Contour type pictures of the distribution of the field components E_θ (left) and E_r (right), taking into consideration the phase. The pictures are for mode $n=3$.
7. The maximum field amplitudes for the fields H_ϕ , E_r , E_θ as a function of the mode number.

Figures

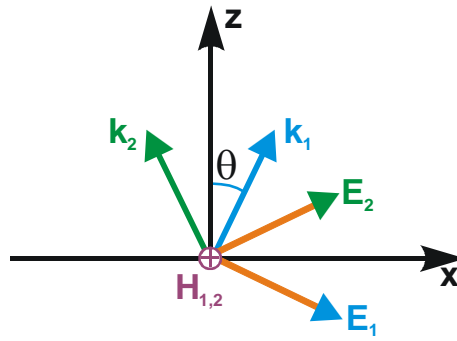


Fig. 1

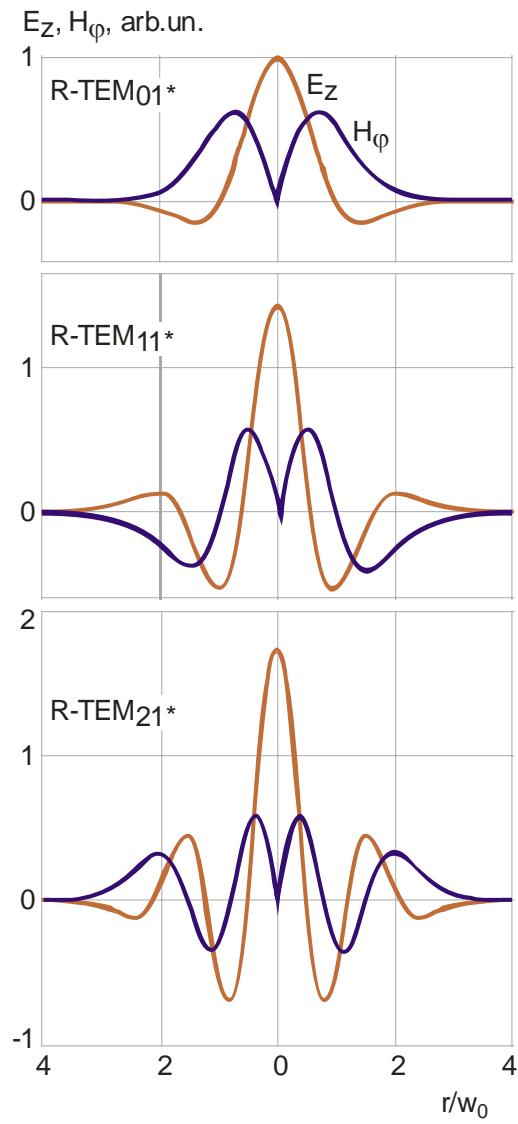


Fig. 2

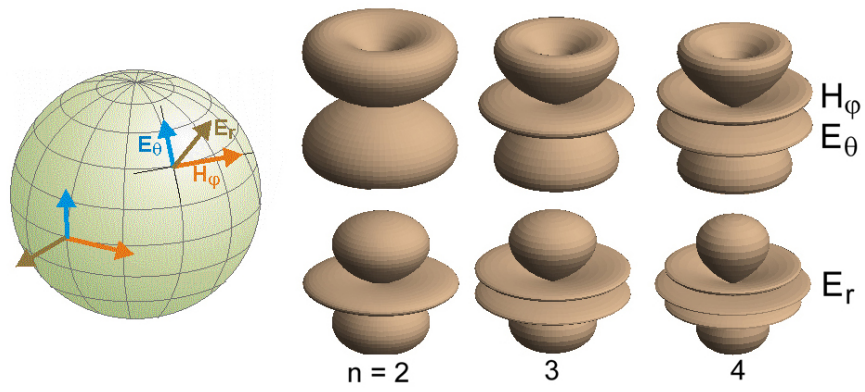


Fig. 3

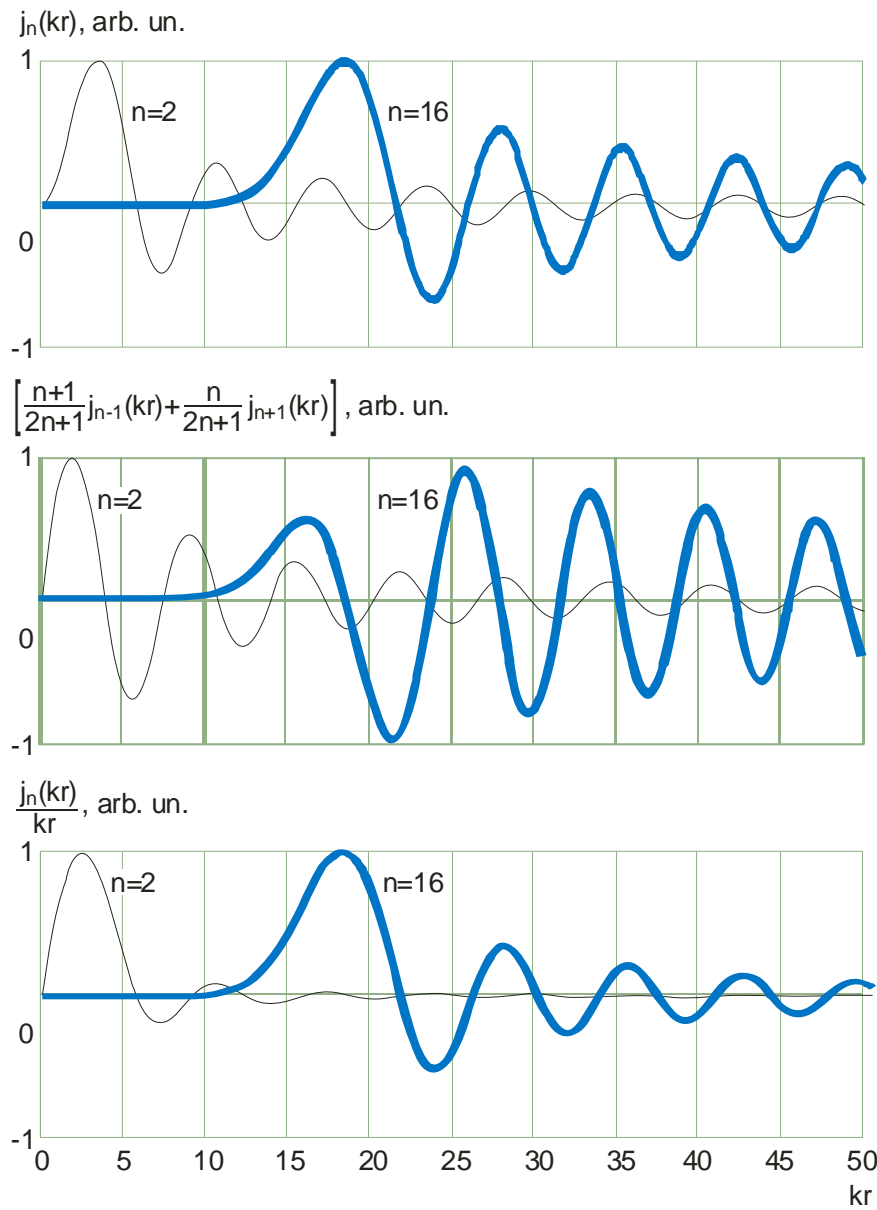


Fig. 4

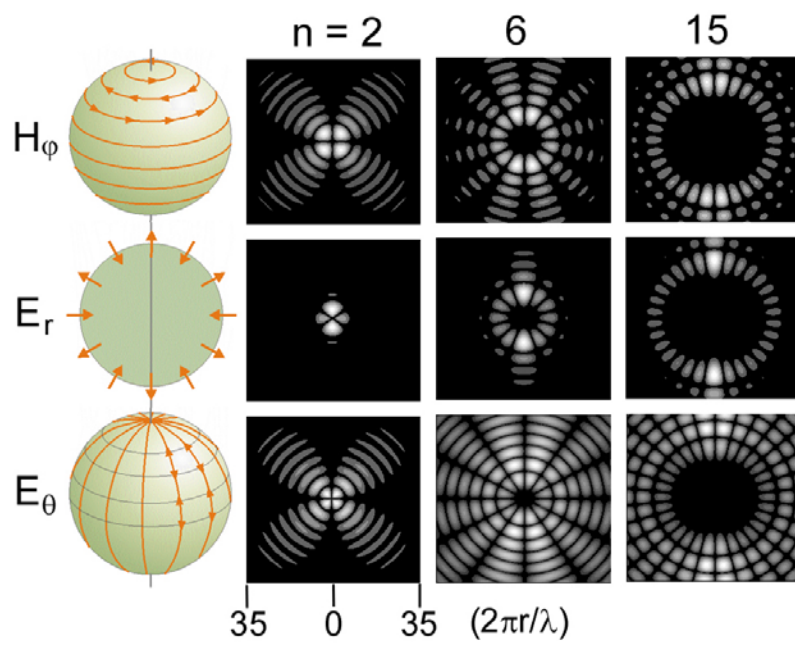


Fig. 5

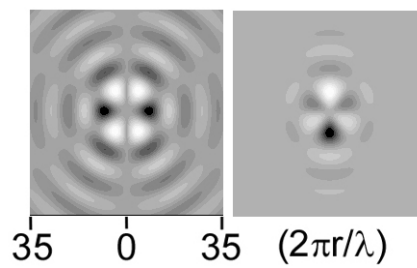


Fig. 6

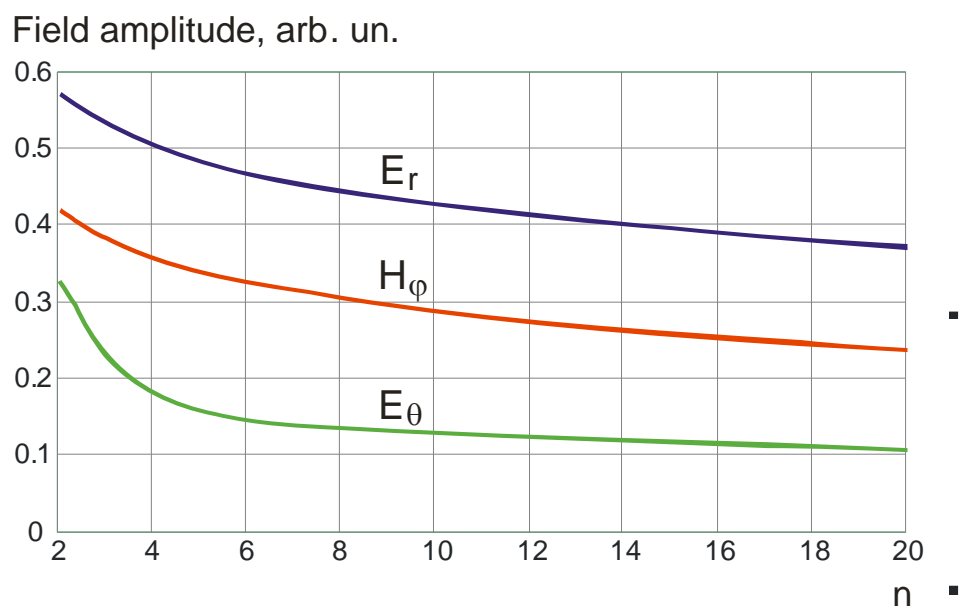


Fig. 7